archives
of thermodynamics
Vol. **38**(2017), No. 3, 23–48
DOI: 10.1515/aoter-2017-0014

Entropy generation and thermodynamic analysis of solar air heaters with artificial roughness on absorber plate

RADHA K. PRASAD*
MUKESH K. SAHU

Department of Mechanical Engineering, National Institute of Technology, Jamshedpur, Jharkhand, India, Pin - 831014

Abstract This paper presents mathematical modelling and numerical analysis to evaluate entropy generation analysis (EGA) by considering pressure drop and second law efficiency based on thermodynamics for forced convection heat transfer in rectangular duct of a solar air heater with wire as artificial roughness in the form of arc shape geometry on the absorber plate. The investigation includes evaluations of entropy generation, entropy generation number, Bejan number and irreversibilities of roughened as well as smooth absorber plate solar air heaters to compare the relative performances. Furthermore, effects of various roughness parameters and operating parameters on entropy generation have also been investigated. Entropy generation and irreversibilities (exergy destroyed) has its minimum value at relative roughness height of 0.0422 and relative angle of attack of 0.33, which leads to the maximum exergetic efficiency. Entropy generation and exergy based analyses can be adopted for the evaluation of the overall performance of solar air heaters.

Keywords: Entropy generation analysis; Entropy generation number; Irreversibility; Bejan number

Nomenclature

A_C	–	collector surface area, m^2
Be	–	Bejan number

*Corresponding Author. Email rkpappnit@gmail.com

C_p	–	specific heat of air, J/(kgK)
D	–	equivalent or hydraulic diameter of duct, m
e	–	rib roughness height, m
Ex_{dest}	–	exergy destruction
Ex_{in}	–	exergy inlet
Ex_{out}	–	exergy outlet
F'	–	collector efficiency factor
F_R	–	collector heat removal factor
G	–	mass flow rate of air per unit collector area, kg/s m^2
H	–	height of duct, m
h	–	heat transfer coefficient, W/m^{2}K
h_w	–	convective heat transfer coefficient due to wind, W/m^{2}K
h_{c-ab-f}	–	convective heat transfer coefficient between absorber plate and fluid, W/m^{2}K
I	–	solar irradiation intensity, W/m^2
K_i	–	thermal conductivity of insulation, W/(m K)
L	–	length of duct, m
L_g	–	cover glass thickness, m
L_1	–	gap between covers, m
M	–	number of glass covers
m	–	mass flow rate of air, kg/s
Ns	–	entropy generation number
Nu$_s$	–	Nusselt number for smooth duct
Nu	–	Nusselt number between flowing fluid and absorber plate
Nu$_{ab-f}$	–	Nusselt number for roughened duct
Q_s	–	energy received by the collector absorber plate from the sun
Q_u	–	useful heat gain, W
P	–	pitch of roughness element, m
P_m	–	mechanical power, W
ΔP	–	pressure drop across the duct, Pa
Pr	–	Prandtl number
Re	–	Reynolds number
St	–	Stanton number
S_{gen}	–	entropy generation, W/K
T	–	temperature, K
ΔT	–	air temperature rise across the duct, K
T_a	–	atmospheric air temperature, K
T_{bp}	–	mean bottom plate temperature, K
T_f	–	mean temperature of fluid, K
T_g	–	temperature of glass cover, K
T_i	–	inlet air temperature, K
T_o	–	outlet air temperature, K
Tp	–	mean absorber plate temperature, K
T_{sun}	–	temperature of sun, K
U_L	–	overall heat loss coefficient, W/m^{2}K
U_t	–	top loss coefficient, W/m^{2}K
U_b	–	bottom loss coefficient, W/m^{2}K
U_s	–	side loss coefficient, W/m^{2}K
V	–	velocity of air in the duct, m/s
V_w	–	wind velocity, m/s
W	–	width of duct, m

Greek symbols

α	–	angle of attack, degree
β	–	tilt angle of collector surface, degree
δ_i	–	insulation thickness , m
ε_p	–	emissivity of absorber plate
ε_g	–	emissivity of glass cover
η_{EN}	–	energy efficiency
η_{eff}	–	effective efficiency
η_{EX}	–	exergy efficiency
η_{II}	–	second law efficiency
μ	–	dynamic viscosity of air, N s/m^2
μ_{th}	–	thermal efficiency
$(\tau\alpha)_e$	–	effective transmittance-absorptance product
ρ_a	–	density of air, kg/m^3
σ	–	Stefan Boltzman's constant , Wm^{-2} K^{-4}

Dimensionless

$\alpha/90$	–	relative angle of attack
e/D	–	relative roughness height
f_r	–	friction factor for roughened duct
f_s	–	friction factor for smooth surface
P/e	–	relative roughness pitch
SAH	–	solar air heater
W/H	–	duct aspect ratio

1 Introduction

The increasing use of energy day-by-day and faster depletion of available conventional and non-recycle fossil fuels has compelled to opt for alternative source of energy and hence there is a need of harnessing energy from various non-conventional energy resources like solar, wind, geothermal, tidal etc. Among all the available non-conventional energy resources, the solar energy is the most promising source because of its free availability, non-polluting and non-depleting nature. However, the major disadvantage of this energy is its irregular availability round the year and spasmodic nature day-wise [1]. Solar air heater has wide applications for heating air at low to moderate temperatures. Due to simple, compact and low cost structure, it is employed for space heating, drying of fruits, seeds and grains, timber seasoning, etc. The main draw back with solar air heater is that heat transfer rate from absorber plate to fluid (air) is poor as the specific heat of air is low thus, heat loss to the surroundings is high [1,2].

Several methods to improve the heat transfer rate from the absorber plate of a solar air heater have been reported [2,3]. To provide artificial

roughness on absorber plate at its air flow side is one of such methods. Several roughness elements with different geometries have been employed by the investigators in order to enhance the heat transfer rate and thereby to have improved overall thermal performance of such solar air heaters (SAH). The evaluation of thermal efficiency is an incomplete measure of performance because it does not take into account all the factors required for evaluation of overall performance of a solar collector [4,5]. Thermal efficiency only accounts for quantity of energy transferred, and can be ambiguous where heat is recovered at low temperatures. Exergy is maximum work, which can be obtained from a system in a quantified manner [6,7]. The study of entropy generation in heat transfer by forced convection in four different flow configurations: pipe flow, flow over a flat plate, single cylinder in cross-flow, and flow in the entrance region of a flat rectangular duct has been made by Bejan [8]. The entropy generation due to heat transfer and due to viscous effect has been investigated in detail by the author.

Entropy generation in different duct geometries: circular, square, equilaterally triangular and rectangular with the aspect ratio of 1/2, and sinusoidal with the aspect ratio of $\sqrt{3}/2$ was studied by Sahin [9]. He determined the optimum duct geometry which minimizes losses for laminar flow at constant heat flux. Sahin [10] studied numerically the effect of variable viscosity on the entropy generation and pumping power in a laminar fluid flow in a duct subjected to constant heat flux and found an optimum duct length which minimizes total energy losses due to both entropy generation and pumping power. Oztop *et al.* [11] studied entropy generation through hexagonal cross-sectional duct for constant wall temperature in laminar flow. Geometrical effect of hexagonal duct was considered. The variation of total entropy generation along the duct length was studied. Dagtekin *et al.* [12] studied the entropy generation analysis in a circular duct with internal longitudinal fins of different shapes for laminar flow. Three different fin shapes, namely thin, triangular and V-shaped ones were chosen for the analysis. Calculations were performed for various lengths and number of fins, temperature difference and fin angle for triangular and V-shaped fins. Ko and Ting [13] analyzed entropy generation induced by forced convection in a curved rectangular duct with external heating by numerical methods for 3D, steady, and laminar flow conditions. The effects of Dean number, external wall heat flux and cross-sectional aspect ratio, on entropy generated from frictional irreversibility and heat transfer irreversibility were

investigated. They reported that the optimal aspect ratio is dependent on heat flux and Dean number.

Numerical investigation on entropy generation in concentric curved annular square ducts under constant wall temperature condition was carried out by Haydar Kucuk [14]. The problem was solved by assuming steady, incompressible and fully developed laminar flow with constant properties of the fluid. It was reported that, the distribution of volumetric entropy generation coming out from the heat transfer irreversibility, is depending on the curvature of the duct. Shahi *et al.* [15] studied, entropy generation due to natural convection of a nanofluid consisting of water and Cu in a cavity with a protruded heat source. It was observed that the maximum value of Nusselt number and minimum entropy generation are obtained when heat source mountains in the bottom horizontal wall. Mahian *et al.* [16] numerically studied the entropy generation and heat transfer rate due to nanofluid flow in a flat plate solar collector. Al_2O_3/water nanofluid with four different particle sizes 25–100 nm and volume concentrations up to 4% have been taken. Effects of tube roughness, nanoparticle size, and different thermophysical models have been investigated on the Nu, h, T_o, entropy generation, and Bejan number. A critical mass flow rate was determined under two different values of solar irradiation and ambient temperature.

Velmurugana and Kalaivanana [17] carried out energy and exergy analyses of multipass flat plate solar air heater. They found higher energy and exergy performances of triple pass solar air heater over the single and double pass solar air heaters. Layek *et al.* [18] carried out their numerical investigation based on the second law of thermodynamics. They evaluated entropy generation number and irreversibility distribution ratio of chamfered rib-groove absorber plate solar air heater. Performance evaluation and entropy generation in the double pass solar air heater with longitudinal fins was investigated by Naphon [19]. Behura *et al.* [20] carried out an outdoor experimental investigation by using 3 sided transverse wire rib roughness with only the bottom side insulated remaining sides made with glass. The overall thermal performance was found to be enhanced as compared to one sided transverse ribs. Kumar *et al.* [21] carried out their experimental investigation by employing multiple V-shape wire ribs with gap on the absorber plate and found better performance as compared to the continuous V-shape ribs. Rybiński and Mikielewicz [28] presented two analytical solutions for friction factor and Nusselt number of fully developed laminar fluid flow in straight mini channels having rectangular cross-section. Zima and

Dziewa [29] developed one-dimensional mathematical model for simulation of transient processes in liquid flat plate solar collector tubes.

The literature reveals that although extensive researches have been performed on the use of artificial roughness on absorber plate but the entropy generation analysis based on the second law of thermodynamics for a solar air heater having its absorber plate roughened with arc shaped wire ribs, has not been worked out in detail. In view of this, a mathematical model has been developed to evaluate entropy generation, entropy generation number, Bejan number and irreversibility of a solar air heater having arc shaped wire ribs as roughness element on underside of the absorber plate of the air heater duct. A comparison has been made with a simple solar air heater working under similar conditions in order to have most appropriate and meaningful values of the design parameters for enhanced overall performance.

2 Mathematical modeling

Figure 1 shows schematic diagram of a solar air heater having arc shaped wire ribs as roughness element at the underside of the absorber plate. The geometry of the roughness on absorber plate has been shown in Fig. 2.

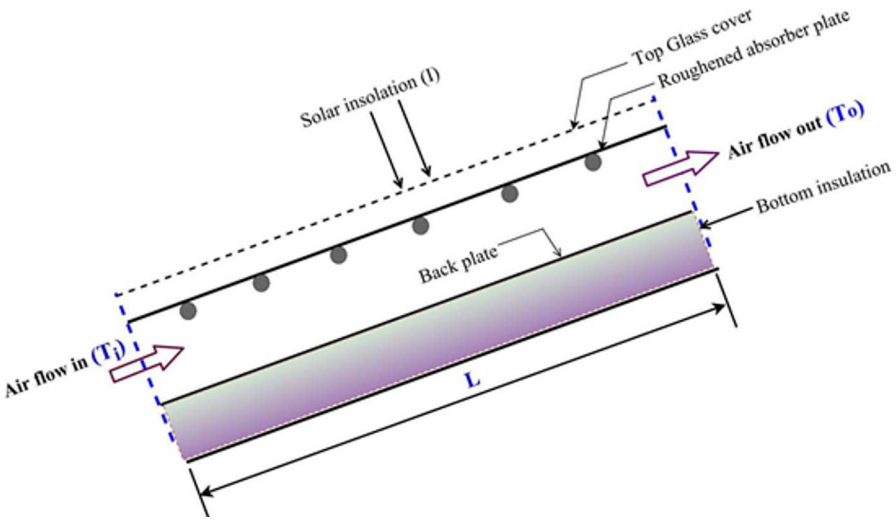

Figure 1: Solar air heater with roughened absorber plate.

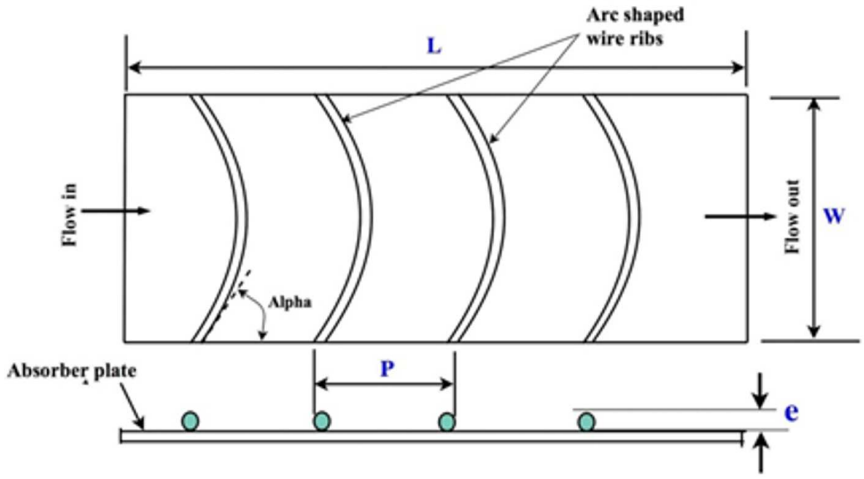

Figure 2: Roughness geometry on absorber plate.

2.1 Evaluation of thermal efficiency

The thermal efficiency of a solar collector is concerned with quantity of useful thermal energy gain and is evaluated, based on the first law of thermodynamics, as [1,2]

$$\eta_{th} = \frac{Qu}{IA_c} = F_R \left[(\tau\alpha)_e - U_L \left(\frac{T_i - T_a}{I} \right) \right] , \tag{1}$$

where F_R is the heat removal factor and it is expressed as

$$F_R = \frac{mC_p}{U_L A_c} \left[1 - \exp \left(\frac{-A_c F' U_L}{mC_p} \right) \right] . \tag{2}$$

The thermal efficiency of a collector using air as the working fluid, can also be given in terms of mass flow rate, specific heat of air and temperature difference of air at outlet and inlet as [1,2]

$$\eta_{th} = \frac{Qu}{IA_c} = \frac{mC_p(T_o - T_i)}{IA_c} . \tag{3}$$

The overall heat loss coefficient (U_L) used in Eq. (1) is calculated by [5,27]

$$U_L = U_b + U_s + U_t . \tag{4}$$

To evaluate the top loss coefficient, U_t, an approximate initial mean plate temperature is assumed and proceeded to find approximate values of U_L, F_R and Q_u [5].

New mean plate temperature is to be calculated as

$$T_P = T_a + \left[\frac{Q_u(1-F_R)}{A_c U_L F_R}\right] . \tag{5}$$

Outlet temperature of air, T_o, can be calculated as

$$T_o = T_i + \frac{Q_u}{m\,C_p} . \tag{6}$$

The collector efficiency factor F' which is the ratio of actual heat collection rate to the useful heat collection rate when the collector plate is at the local fluid temperature, can be calculated as

$$F' = \frac{h}{h+U_L} , \tag{7}$$

where h is the effective heat transfer coefficient.

2.2 Performance analysis of solar collector based on second law of thermodynamics

Exergy efficiency evaluation, based primarily on the second law of thermodynamics, is a better approach than that of energy efficiency evaluation Eq. (1) for performance analysis of a solar collector as the former takes both into account the quality and quantity of the energy transferred.

Under steady flow condition and treating air as an ideal gas having constant specific heat with negligible humidity, exergy balance equation can be expressed as:

$$\sum Ex_{in} - \sum Ex_{out} = Ex_{dest} . \tag{8}$$

The inlet exergy, Ex_{in}, of absorbed heat from solar radiation is given by

$$Ex_{in} = \left(1 - \frac{T_a}{T_{sun}}\right) Q_s , \tag{9}$$

where Q_s is the energy received by the collector absorber plate from the sun and is given by

$$Q_s = I A_c (\tau\alpha)_e . \tag{10}$$

The outlet exergy, Ex_{out}, includes exergy of outlet fluid

$$Ex_{out} = mC_p(T_o - T_i) + mC_pT_a \ln\left(\frac{T_o}{T_i}\right) + mRT_a \ln\left(\frac{P_{out}}{P_{in}}\right) . \tag{11}$$

In the right side of Eq. (11) the first term represents the variation in enthalpy of air flowing through the collector duct while the mid-term represents the entropy created due to change in temperature of air $(S_{gen})_H$ and the last term represents the entropy created due to pressure drop $(S_{gen})_P$ in the duct.

By combining Eqs. (9), (10) and (11) and substituting into Eq. (8), the resulting relation is obtained as

$$Ex_{dest} = \left(1 - \frac{T_a}{T_{sun}}\right) IA_c(\tau\alpha)_e - mC_p\,(T_o - T_i) - mC_p\,T_a \ln\left(\frac{T_o}{T_i}\right) - m\,RT_a\,\ln\left(\frac{P_{out}}{P_{in}}\right) . \tag{12}$$

The irreversibility, I_{rev}, expressed in the following form [17,18]

$$I_{rev} = T_a\,S_{gen} . \tag{13}$$

Entropy generation number, Ns, is given by

$$Ns = \frac{I_{rev}}{Q_s} , \tag{14}$$

and Bejan generation number, Be, is given by [22]

$$\mathrm{Be} = \frac{(Ns)_H}{(Ns)_H + (Ns)_P} , \tag{15}$$

where $(Ns)_H$ is entropy generation number due to heat transfer and $(Ns)_P$ is entropy generation number due to pressure drop (friction) in the duct.

The second law efficiency (exergetic efficiency) of solar air heater is given as [17]

$$\eta_{II} = \frac{Ex_{out}}{Ex_{in}} . \tag{16}$$

2.3 Entropy generation analysis of solar collector

There are two sources of entropy generation in a solar collector for heating air [6–8,22–25]. The first entropy generation is due to loss of energy owing to the friction between the collector surface and the air flowing through it, and the second one is due to the heat transfer or temperature change in the heat carrier fluid (air).

Entropy generation, S_{gen}, by considering pressure drop in the collector duct, is given by

$$S_{gen} = \frac{1}{T_a} I_{rev} \ . \tag{17}$$

Dittus –Boelter equation has been used to calculate convective heat transfer coefficient between flowing fluid and conventional smooth plate solar air heater

$$h_{c-ab-f} = \mathrm{Nu}_{ab-f} \frac{K}{D} \ , \tag{18}$$

where Nu_{ab-f} is the Nusselt number for smooth plate solar air heater duct for $\mathrm{Re} \geq 2300$ given by [5]

$$\mathrm{Nu}_{ab-f} = 0.024(\mathrm{Re})^{0.8}(\mathrm{Pr})^{0.4} \ . \tag{19}$$

In the case of laminar flow ($\mathrm{Re} < 2300$) the following correlation for the case of smooth plate solar air heater duct is used [17]:

$$\mathrm{Nu}_{ab-f} = 4.9 + \frac{0.0606 \left(\mathrm{RePr}\frac{D}{L}\right)^{0.5}}{1 + 0.0909 \left(\mathrm{RePr}\frac{D}{L}\right)^{0.7} (\mathrm{Pr})^{0.17}} \ . \tag{20}$$

For a solar air heater duct having wires as roughness elements in arc shape on the absorber plate, the convective heat transfer coefficient between flowing fluid and absorber plate is calculated by using the correlation [26]

$$\mathrm{Nu}_{ab-f} = 0.001047(\mathrm{Re})^{1.3186} \left(\frac{e}{D}\right)^{0.3772} \left(\frac{\alpha}{90}\right)^{-0.1198} \ . \tag{21}$$

The equivalent or hydraulic diameter D of the duct is given by

$$D = \frac{2(W \times H)}{(W + H)} \ . \tag{22}$$

The Reynolds number of the flow in the duct is given by

$$\mathrm{Re} = \frac{GD}{\mu} \ , \tag{23}$$

where the mass velocity, G, is given by

$$G = \frac{m}{WH} \ . \tag{24}$$

2.4 Pressure drop and mechanical power

In the present analysis the correlation, proposed by Saini and Saini [26] to calculate the friction factor for roughened air heater duct has been used:

$$f_r = 0.14408\mathrm{Re}^{-0.17103}\left(\frac{e}{D}\right)^{0.1765}\left(\frac{\alpha}{90}\right)^{0.1185} \tag{25}$$

and friction factor for smooth plate solar air heater duct is evaluated using the correlation given by

$$f_s = 0.085\mathrm{Re}^{-0.25} \, . \tag{26}$$

The loss of pressure, ΔP, in the air heater duct is calculated as

$$\Delta P = \frac{2\, f\, L\, V^2\, \rho_a}{D} \, . \tag{27}$$

The mechanical power, P_m, needed to overcome the energy loss associated with the pressure drop can be calculated as

$$P_m = \frac{m\Delta P}{\rho_a} \, . \tag{28}$$

2.5 Solutions of performance of solar air heater

The thermal efficiency and entropy generation of roughened solar air heater duct and also that of conventional type for various mass flow rates and solar irradiations have numerically been calculated using collector configuration (Fig.1) and system properties and operating conditions according to Tab. 1. In the present work, the ambient temperatures, T_a, and inlet air temperature, T_i, have been considered as same. In order to determine the top loss coefficients, U_t, an assumed value of mean plate temperature, T_p, is made by using Eq. (5) with approximate values of the heat removal factor, plate efficiency factor and useful heat energy gain are evaluated.

If the new calculated temperature, T_p, of the plate differs by more than 0.0001 from its initial value, then this new temperature is used as the initial temperatures in Eq. (5) for the next iteration and the process is kept continued till an optimum new temperature is obtained with maximum $\pm 0.01\%$ deviation of its respective input values and accordingly the relevant parameters are calculated. In order to obtain the thermal efficiency Eq. (3), second law efficiency Eq. (16), and entropy generation Eq. (17) numerically, programming codes have been developed in MATLAB software

environment. The flow chart of the executed program to obtain various parameters is also shown in Fig. 3a.

Table 1: Typical values of system and operating parameters used in presented investigation.

Parameters	Range/base value(s)
Collector dimensions	
Collector length (L), m	1.5
Collector width (W), m	1.0
Duct depth (H), m	0.030
Gap between absorber plate and glass cover (L_1), m	0.05
Absorber plate	
Emissivity of absorber plate (ε_P), dimensionless	0.9
Glass cover	
Number of glass covers (M), dimensionless	1.0
Emissivity of glass cover (ε_g), dimensionless	0.88
Thickness of glass cover (L_g), m	0.004
Effective transmittance absorptance product $\tau\alpha_e$, dimensionless	0.85
Insulation	
Thermal conductivity of insulation (K_i), W/m K	0.037
Thermal conductivity of glass (K_g), W/m K	0.75
Thickness of insulation (δ_i), m	0.05
Relative roughness height (e/D), dimensionless	0.0256–0.0422
Relative roughness pitch (P/e), dimensionless	10
Relative angle of attack ($\alpha/90$), dimensionless	0.33–0.66
Operating parameters	
Atmospheric air temperature (T_a), K	300
Velocity of wind (V_w), m/s	1.5
Reynolds number (Re)	1650–21500
Solar irradiation (I), W/m^2	600–1000

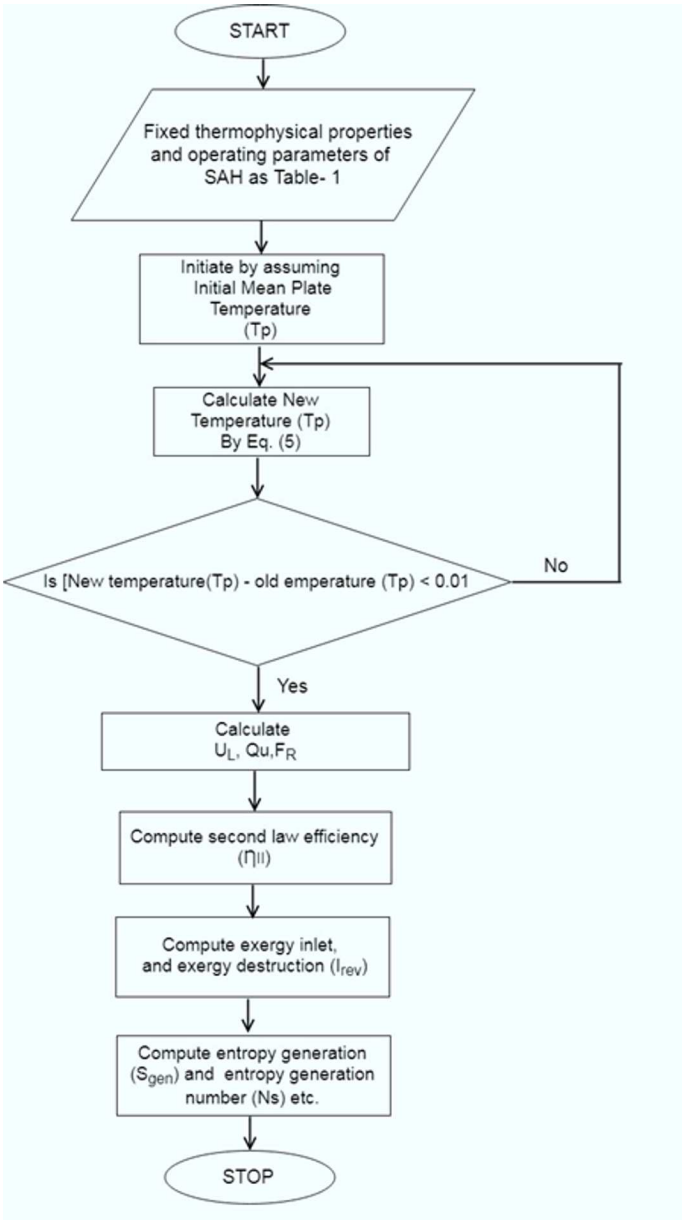

Figure 3: (a) Flow chart for theoretical solution procedure.

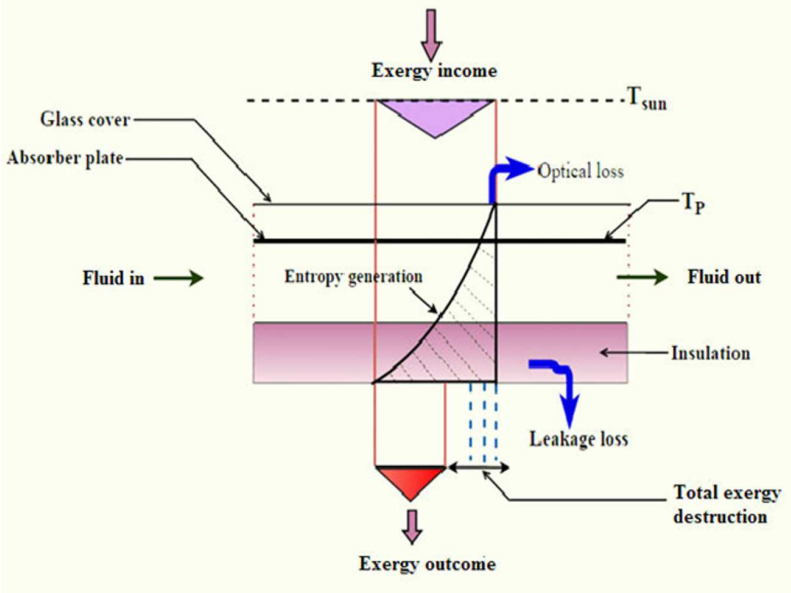

Figure 3: (b) Exergy inflow, entropy generation process and various losses in a solar air heater.

3 Results and discussion

Entropy generation, S_{gen}, entropy generation number, Ns, irreversibility, I_{rev}, or exergy destruction and Bejan number, Be, were calculated and plotted as a function of Reynolds number, Re, covering the entire range of operating and system parameters, given in Tab. 1 Exergy efficiencies account for the temperatures associated with energy transfers to and from solar air heater, and consequently provide a measure of how solar collector nearly approaches to ideal efficiency.

3.1 Effect of relative roughness height and relative angle of attack on entropy generation

Figure 4 shows the plots of entropy generation, S_{gen}, as a function of Reynolds number Re with various values of e/D for roughened solar air heater and also of conventional type. The fixed parameters were taken as $P/e = 10$, $\alpha/90 = 0.33$, and $I = 850$ W/m^2. The entropy generation has been calculated by considering the pressure drop by using Eqs. (12) and (17). It is found from Fig. 4 that, the S_{gen} continues to increase with the

increase in Reynolds number for both, i.e., rough and smooth flat plate solar air heaters. Entropy generation values is the highest for the smallest value of $e/D = 0.0256$ and the lowest at highest value of $e/D = 0.0422$ (used for present analysis). The value of entropy generation for smooth plate solar air heating (SAH) duct is lower than the roughened type, for all values of Re. The trend of variation of entropy generation for both types of heaters are similar. The values of S_{gen} at Re = 22956 is 3.3 W/K and 2.68 respectively for roughened ($e/D = 0.0256$, $P/e = 10$, $\alpha/90 = 0.33$) and smooth plate SAHs, hence it can be said that, S_{gen} for roughened duct is 22.85% more as compared to smooth plate SAH. From the above results it can also be concluded that, the S_{gen} decreases with increase in e/D.

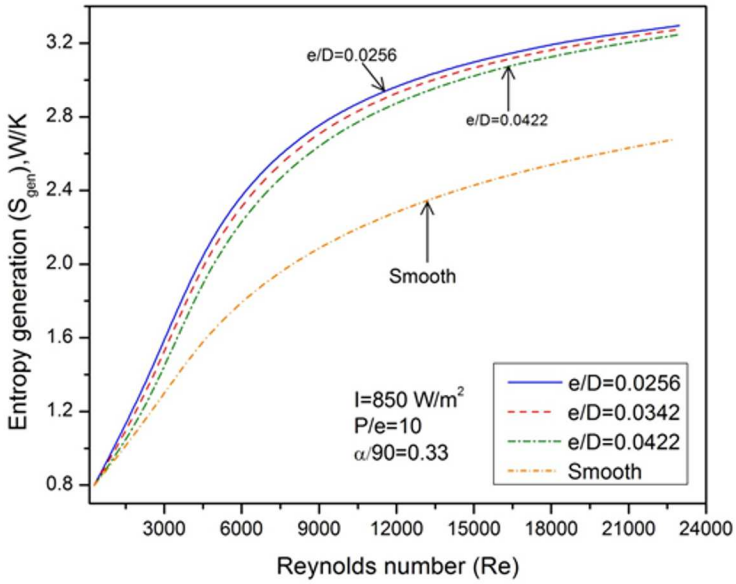

Figure 4: Variation of entropy generation with Reynolds number at different relative roughness height.

Figure 5 exhibits the variation of S_{gen} as a function of Re and different values of relative angle of attack ($\alpha/90$) for arc shape wire rib roughened and also flat plate solar air heater for $T_i = 300$ K. The fixed parameters was taken as $P/e = 10$, $e/D = 0.0422$ and $I = 850$ W/m^2. From Fig. 5 it can be observed that, S_{gen} is found to be increasing with Re for roughened and flat plate solar air heaters. Furthermore it can be seen that S_{gen} values of roughened solar air heater with $\alpha/90 = 0.66$ is higher as compared to

the values obtained at $\alpha/90 = 0.33$ and conventional solar air heater for all values of Re. On the basis of above results it can be concluded that the entropy generation can be minimized by using/employing $\alpha/90 = 0.33$ for the present roughened solar air heater which leads into maximization of second law exergetic efficiency.

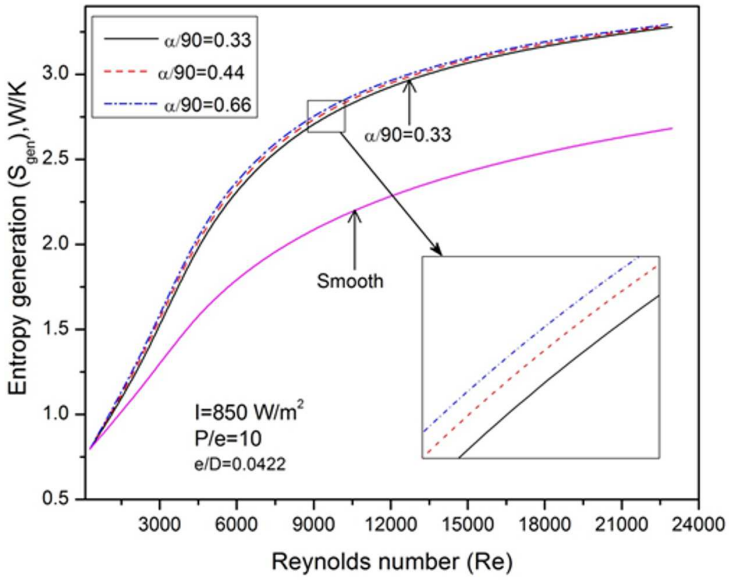

Figure 5: Variation of entropy generation with Reynolds number at different relative angle of attack.

3.2 Effect of roughness parameters on entropy generation number

Figures 6 and 7 shows the effect of three different e/D and $\alpha/90$ values on dimensionless entropy generation number of roughened and simple solar air heaters as a function of Re. The fixed parameters were taken as shown in Fig. 6. It can be observed from Fig. 6 that Ns is found to be increases as values of Re increased, this tendency is followed by both SAHs. The values of Ns is decreases as the value of e/D increases, i.e., the values of Ns for $e/D = 0.0422$ is having lower as compared to $e/D = 0.0256$. However the values of Ns for smooth SAH is lower as compared to roughened duct for all values of Re.

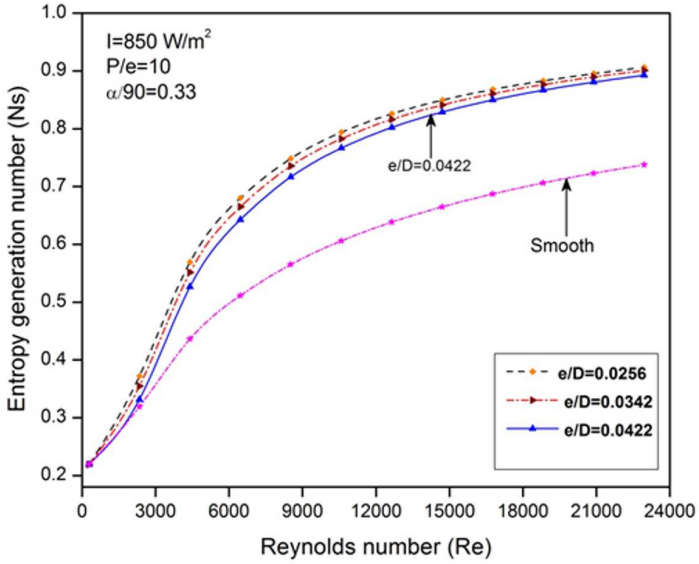

Figure 6: Variation of entropy generation number, Ns, with Re at different e/D.

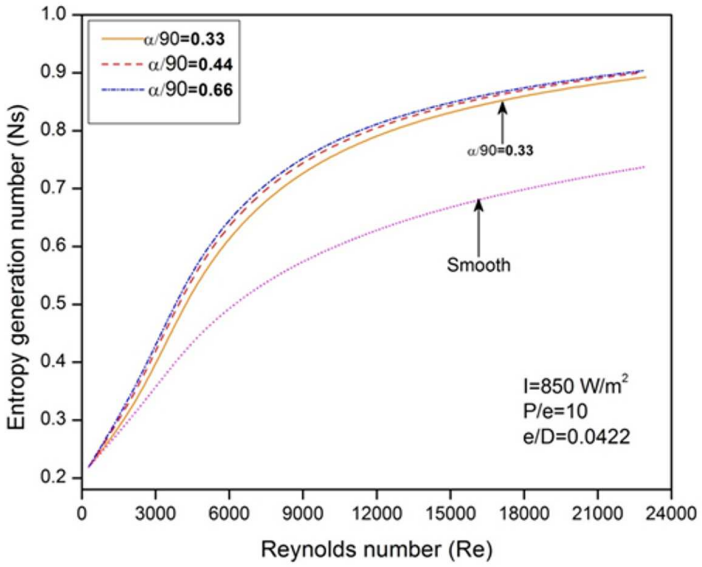

Figure 7: Variation of entropy generation number, Ns, with Re at different $\alpha/90$.

Figure 7 depicts that similar increasing trend is followed by Ns as a function of Re for all three values of $\alpha/90$ for rough and smooth SAHs. The values of Ns is smaller for $\alpha/90 = 0.33$ as compared to $\alpha/90 = 0.44$ and $\alpha/90 = 0.66$. On the other hand smooth SAH is having lower values of Ns as compared to all values of $\alpha/90$ and Re.

3.3 Effect of roughness parameters on irreversibility

Figures 8 and 9 have been drawn in order to show the influence of e/D and $\alpha/90$ values on irreversibility, I_{rev}, of roughened and simple solar air heaters as variation in the values of Re. The fixed parameters such as $P/e = 10$, and $I = 850$ W/m^2 remains unchanged.

As expected, I_{rev}, is having tendency to increase with growth in the values of Re for both SAHs. It happens due to the fact that I_{rev} is product of ambient temperature, T_a, and entropy generation, S_{gen}, (refer Eq. (13)) where S_{gen} is the function of heat transfer and pressure drop (friction) in the duct, as the Re increases these two parameters a increase.

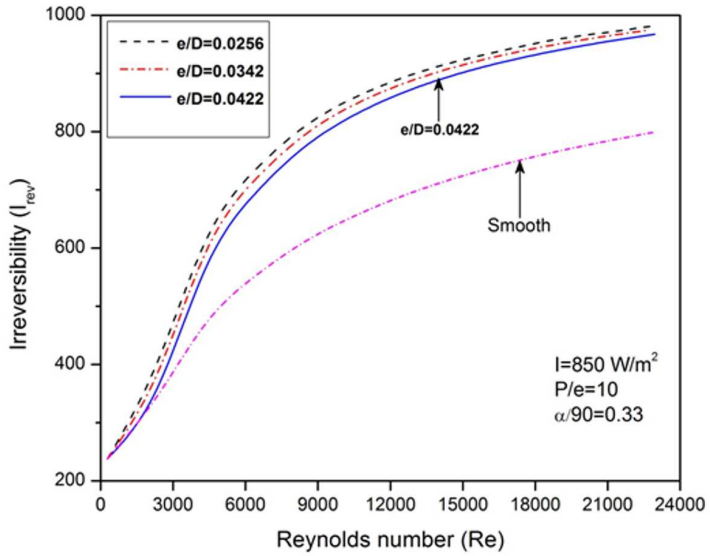

Figure 8: Irreversibility as a function of Reynolds number for different values of e/D.

It is clear from Fig. 9 that, I_{rev} (exergy destruction) increases continuously with increasing Re. The value of irreversibility at $\alpha/90 = 0.66$ is higher as compared to at $\alpha/90 = 0.33$ and 0.44 for all Re. The variation of I_{rev}

and second law efficiency with Re for arc shaped wire roughened solar air heater has been given in Tab. 2. The I_{rev} increases with Re whereas second law efficiency increases upto certain Re.

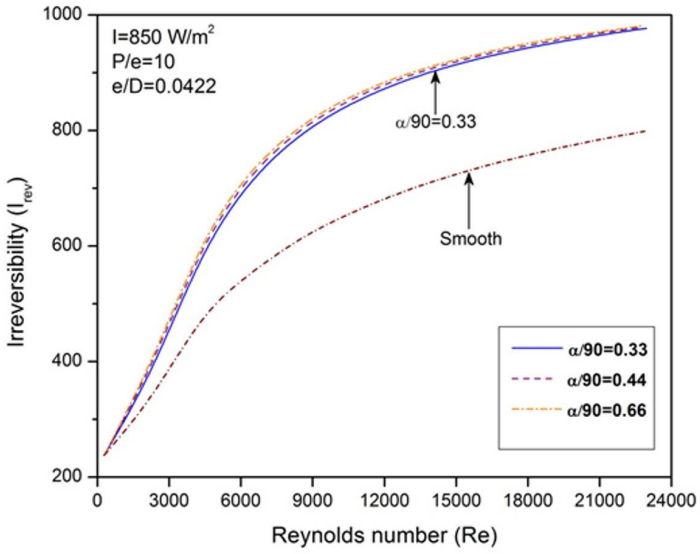

Figure 9: Irreversibility as a function of Reynolds number for different values of $\alpha/90$.

4 Entropy generation and second law efficiency comparison

Figure 10a shows the comparison of S_{gen} and second law efficiency, η_{II}, for roughened SAH with variation in the values of Re. It can be seen from Fig. 10 that second law efficiency increases with Re upto its optimal value ($\eta_{II} = 2.52\%$, Re = 6460). After passing this critical value of Reynolds number it is exhibiting the decreasing trend. The η_{II} decreases after critical Re. This occurs due to the reason that with increasing Re various losses (like optical loss, leakage loss, friction etc.), as shown in Fig. 3b go on increasing and attribute to the increase in S_{gen} and lowering of second law efficiency. It is imperative to select the various parameters like the duct depth, H, and solar irradiation, I, etc., for reduced S_{gen} and to get optimum useful energy, Q_u, or quality energy efficiency, i.e., η_{II}.

Table 2: Results of irreversibility and second law efficiency of solar air heater with arc shaped wire roughness at $I = 850$ W/m^2 and Re = 270–23.000.

Parameter		Reynolds		Exergy	Second law
e/D	$\alpha/90$	number	Irreversibility	loss (%)	efficiency (%)
0.0422	0.33	274	237.47	98.98	1.01
		2336	358.73	98.06	1.93
		4398	570.16	97.50	2.49
		6460	696.24	97.48	2.51
		8522	776.26	97.61	2.38
		10584	830.46	97.80	2.19
		12646	869.23	98.01	1.98
		14708	898.26	98.23	1.76
		16770	920.87	98.48	1.51
		18832	939.11	98.76	1.23
		20894	954.28	99.07	0.92
		22956	967.30	99.41	0.58

Furthermore another result can be obtained from Fig. 10a that S_{gen} is having increasing trend with growth in the values of Re (as already discussed in previous section). The variation in S_{gen} and η_{II} with Re has been plotted in Fig. 10b for roughened and smooth plate solar air heaters for the fixed values of the parameter with $P/e = 10$, $e/D = 0.0422$, $\alpha/90 = 0.33$ with inlet temperature $T_i = 300$ K and $I = 850$ W/m^2.

From the plot it is found that the S_{gen} has the increasing tendency with increase of Re for both, i.e., rough and smooth absorber plate solar air heaters, but the entropy generation values for smooth and rough solar collectors having same values of S_{gen} upto Re = 2500 (approx.). In other words, it can be said that upto Re = 2500 there is no effect of the roughness rib on the absorber and it acts like solar air heater of conventional type that is the absorber plate without roughness. For Re $<$ 2500 (approx.) there is no significant difference of entropy generation between the smooth plate and roughened absorber plate solar air heaters. Another result of the graph indicates that second law efficiency values is higher for the conventional solar air heater for Re $>$ 21 000 (approx.) over the roughened solar air heater and it follows the same trend as the rough solar air heater.

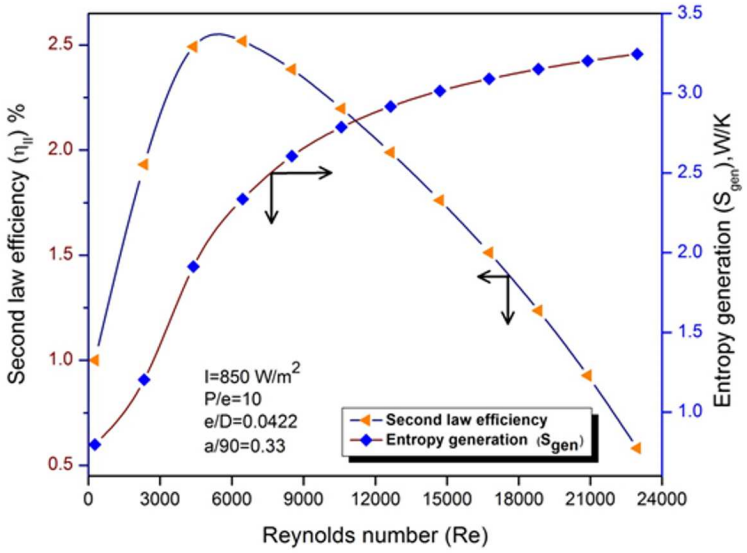

Figure 10: (a) Variation of second law efficiency and entropy generation with Re for roughened solar air heater for roughness parameters $P/e = 10$, $e/D = 0.0422$, $\alpha/90 = 0.33$, $T_i = 300$ K and Insolation $I = 850$ W/m^2.

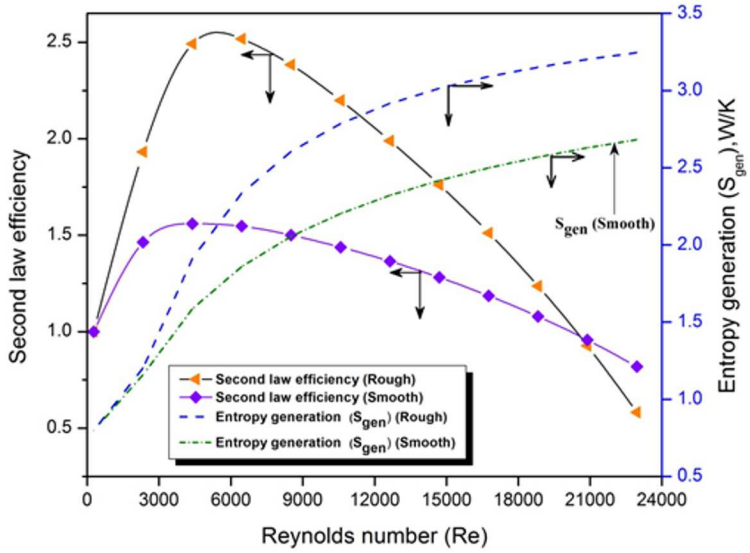

Figure 10: (b) Variation of entropy generation and second law with Re for roughened and smooth plate solar air heaters for roughness parameters $P/e = 10$, $e/D = 0.0422$, $\alpha/90 = 0.33$, and insolation $I = 850$ W/m^2.

4.1 Effect of roughness parameters on Bejan number

The effect of variations in e/D and $\alpha/90$ on Bejan number, Be, as a function of Re has been plotted in Figs. 11 and 12 respectively. From the plot (Fig. 11) it is found that Be has the decreasing tendency with increase in Re for both, i.e., roughened and smooth absorber plate solar air heaters, but Be having same values for both collectors upto Re = 6.000 (approx.). Another result can be obtain from the curves that Be values of $e/D = 0.0422$ is lower as compared to $e/D = 0.0256$ and conventional SAH for Re < 6.000 (approx.). In other words as we increase the Re the Be is decreasing sharply from one (unity) toward zero. It means the entropy generation number due to pressure drop/friction Ns_p in the duct is more dominating over the entropy generation number due to heat transfer Ns_h.

This behavior is due to the fact that the highest value of e/D (in the present investigation $e/D = 0.0422$) produces more barrier in the flow consequently delivering highest friction factor, hence values of Be are lower as compared to other e/D and smooth plate SAH.

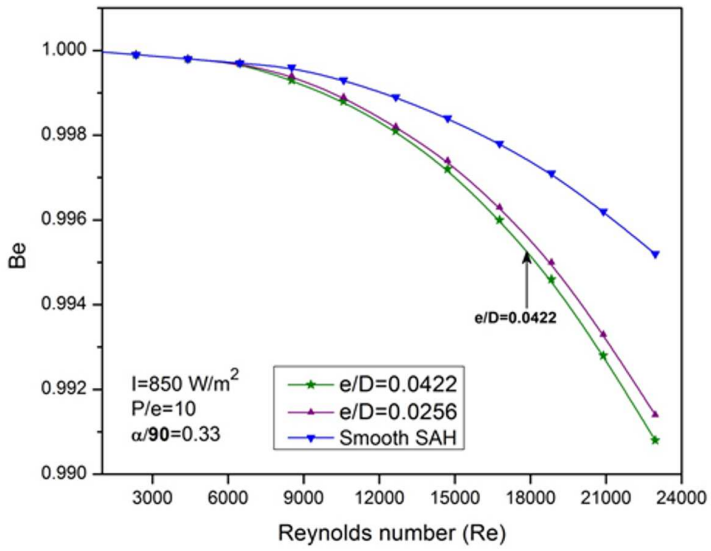

Figure 11: Effect of e/D on Bejan number and comparison of roughened with simple solar air heater as a function of Re.

Figure 12 shows the influence of roughness parameter $\alpha/90$ on Be as function of Re. Similar decreasing trend is obtained for both SAHs with increase in the values of Re. The values of Be for $\alpha/90 = 0.33$ is lower as

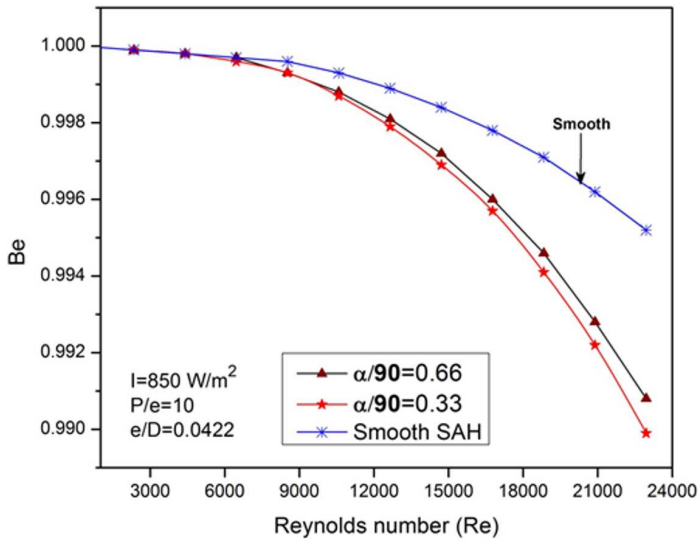

Figure 12: Effect of $\alpha/90$ on Bejan number and comparison of roughened with simple solar air heater as a function of Re.

compared to $\alpha/90 = 0.66$ and simple SAH after Re < 6.000 (approx.). The $\alpha/90 = 0.33$ is having lowest value of Be because at this value of inclination it produces highest friction in the flow.

5 Conclusions

This article presents the comprehensive entropy generation analysis and evaluation of second law efficiency using the principle of second law of thermodynamics, for a solar air heater having arc shape wire roughened absorber plate. The emphasis has been given to analyse entropy generation and to study the effects of roughness parameters viz. relative roughness height, e/D, relative roughness pitch, P/e, and relative angle of attack $\alpha/90$ and also operating parameters, e.g., Reynolds number, solar irradiation on the entropy generation. The following conclusions can be drawn:

- The second law efficiency increases with increase in Re upto its maxima, however at the higher values of Re smooth plate solar air heater is more efficient in comparison to roughened solar air heater. Highest η_{II} is obtained as 2.51 % for roughened solar air heater at Re = 6460

and $I = 850$ W/m^2 while for smooth plate SAH it is having 1.56% for Re $= 4398$ and $I = 850$ W/m^2.

- Entropy generation, entropy generation number and irreversibility increase continuously with increase in the Reynolds number. This trend is followed by both the roughened and smooth absorber plate solar air heaters. The entropy generation is minimum at relative roughness height of 0.0422 and relative angle of attack of 0.33, and relative roughness pitch of 10 which leads into the maximum second law efficiency. Bejan number is having decreasing trend with increase in the values of Reynolds. Minimum is obtained at relative roughness height of 0.0422, relative angle of attack of 0.33, and relative roughness pitch of 10 in the case of rough SAH.

Received 13 November 2016

References

[1] Duffie J.A., Beckman W.A.: *Solar Engineering of Thermal Processes*, 2nd Edn., John Wiley, New York 1991.

[2] Sukhatme S.P., Nayak J.P.: *Solar Energy.* 3rd Edn., Tata McGraw Hill, New Delhi 2011.

[3] Prasad R.K.: *Thermal Performance Characteristics of Unidirectional Flow Porous Bed Solar Energy Collectors for Heating Air.* Ph.D. thesis, Indian Institute of Technology, Roorkee 1991.

[4] Prasad R.K, Saini J.S.: *Packed-bed solar air heater with unidirectional flow arrangement.* In: Proc. Nat. Sem. on Energy Conversion in Buildings, The Institute of Engineers, I.I.T., Roorkee 1992, 29–33.

[5] Sahu M.K., Prasad R.K.: *Exergy based performance evaluation of solar air heater with arc shaped wire roughened absorber plate.* Renew. Energ. **96**(2016), 233–243.

[6] Bejan A.: *Advanced Engineering Thermodynamics.* Wiley Interscience, 1988.

[7] Bejan A.: *Entropy Generation Minimization.* CRC Press, New York 1996.

[8] Bejan A.: *A study of entropy generation in fundamental convective heat transfer.* J. Heat Transfer **101**(1979), 4, 718–725.

[9] Sahin A.Z.: *Irreversibilities in various duct geometries with constant wall heat flux and laminar flow.* Energ. **23**(1998), 6, 465–473.

[10] A.Z. Sahin: *The effect of variable viscosity on the entropy generation and pumping power in a laminar fluid flow through a duct subjected to constant heat flux.* Heat Mass Transfer **35**(1999), 6, 499–506.

[11] Oztop H.F., Sahin A.Z., Dagtekin I.: *Entropy generation through hexagonal cross-sectional duct for constant wall temperature in laminar flow.* Int. J. Energy Res. **28**(2004), 8, 725–737.

[12] Dagtekin I., Oztop H.F., Sahin A.Z.: *An analysis of entropy generation through a circular duct with different shaped longitudinal fins for laminar flow.* Int. J. Heat Mass Tran. **48**(2005), 1, 171–181.

[13] Ko T.H., Ting K.: *Entropy generation and optimal analysis for laminar forced convection in curved rectangular ducts: A numerical study.* Int. J. Therm. Sci. **45**(2006), 2, 138–150.

[14] Haydar Kucuk: *Numerical analysis of entropy generation in concentric curved annular ducts.* J. Mech. Sci. Technol. **24**(2010), 9, 1927–1937.

[15] Mina S., Mahmoudi A.H., Raouf A.H.: *Entropy generation due to natural convection cooling of a nanofluid.* Int. Commun. Heat Mass **38**(2011), 7, 972–983.

[16] Omid M., Kianifar A., Sahin A.Z.,Somchai W.: *Entropy generation during Al_2O_3/water nanofluid flow in a solar collector: Effects of tube roughness, nanoparticle size, and different thermophysical models.* Int. J. Heat Mass Tran. **78**(2014), 64–75.

[17] Velmurugana P., Kalaivanana R.: *Energy and exergy analysis of multi pass flat plate solar air heater — An analytical approach.* Int. J. Green Energy **12**(2015), 8, 810–820.

[18] Layek A., Saini J.S., Solanki S.C.: *Second law optimization of a solar air heater having chamfered rib–groove roughness on absorber plate.* Renew. Energ. **32**(2007), 12, 1967–1980.

[19] Naphon P.: *On the performance and entropy generation of the double-pass solar air heater with longitudinal fins.* Renew. Energ. **30**(2005), 9, 1345–1357.

[20] Behura A.K., Prasad B.N., Prasad L.: *Heat transfer, friction factor and thermal performance of three sides artificially roughened solar air heaters.* Solar Energy **130**(2016), 46–59.

[21] Kumar A., Saini R.P., Saini J.S.: *Development of correlations for Nusselt number and friction factor for solar air heater with roughened duct having multi v-shaped with gap rib as artificial roughness.* Renew. Energ. **58**(2013), 151–163.

[22] Sciacovelli A., Verda V., Sciubba E.: *Entropy generation analysis as a design tool — a review.* Renew. Sustain. Energy Rev. **43**(2015), 1167–1181.

[23] Rosen M.A.: *Second law analysis, approaches and implications.* Int. J. Energy Res. **23**(1991), 5, 415–429.

[24] Bejan A., Kearney D.W., Kreith F.: *Second law analysis and synthesis of solar collector systems.* J. Sol. Energ-T ASME **103**(1981), 1, 23–28.

[25] Incropera F.P., DeWitt D.P.: *Fundamentals of heat and mass transfer.* 5th Edn., John Wiley & Sons, New York 2006.

[26] Saini S., Saini R.P.: *Development of correlations for Nusselt number and friction factor for solar air heater with roughened duct having arc-shaped wire as artificial roughness.* Sol. Energy **82**(2008), 12, 1118–1130.

[27] Malhotra A., Garg H.P., Palit A.: *Heat loss calculation of flat plate solar collectors.* J. Therm. Energ. **2**(1981), 2, 59–62.

[28] Rybiński W., Mikielewicz J.: *Analytical solutions of heat transfer for laminar flow in rectangular channels.* Arch. Thermodyn. **35**(2014), 4, 29–42.

[29] Zima W., Dziewa P.: *Mathematical modelling of heat transfer in liquid flat-plate solar collector tubes.* Arch. Thermodyn. **31**(2010), 2, 45–62.